Supporting Information:

Photophysics of Heme Cyanide: Photodissociation in Ferric Myoglobin Studied by Resonance Raman Spectroscopy

Weiqiao Zeng, Yuhan Sun, Abdelkrim Benabbas and Paul M. Champion*

Department of Physics and Center for Interdisciplinary Research on Complex Systems, Northeastern University, Boston, Massachusetts 02115

*Address correspondence to Paul M. Champion, Tel.: 617-373-5705; E-mail: champ@neu.edu

I. Supporting Data

We have studied the power dependence of MbCN at a lower concentration ratio of CN (10:1) than the 20:1 ratio shown in the main text. The spectra for this alternative study are given in Fig. S1. We also measured the optical absorption spectra of met Mb and the MbCN sample before and after the Raman measurements as shown in Fig. S2.

We find that diffusion has a negligible effect on the MbCN population recovery within the laser focal region being probed by resonance Raman scattering. We have varied the entrance slit width from 20 μm to 100 μm at 26 mw incident laser power and a change in the relative population of metMb is not observed (see Fig. S4). This supports the conclusion that angular diffusion, perpendicular to the optical axis, is not significant within the photostationary conditions used in these measurements. We also present a simple model that helps to estimate the importance of radial diffusion within the spinning cylindrical sample cell. The radial diffusion could conceivably compete with the slow bimolecular rebinding that recovers the MbCN population within the laser focal volume. However, the experiments reported in the main text, which show a nearly inverse dependence of the fitting parameter (*b*) on the CN concentration, demonstrate that bimolecular rebinding is the main channel for MbCN population recovery. Nevertheless, we present the details of the diffusion calculations in the spinning cell in the event they may be of use in other applications involving slower processes or slower spinning speeds.

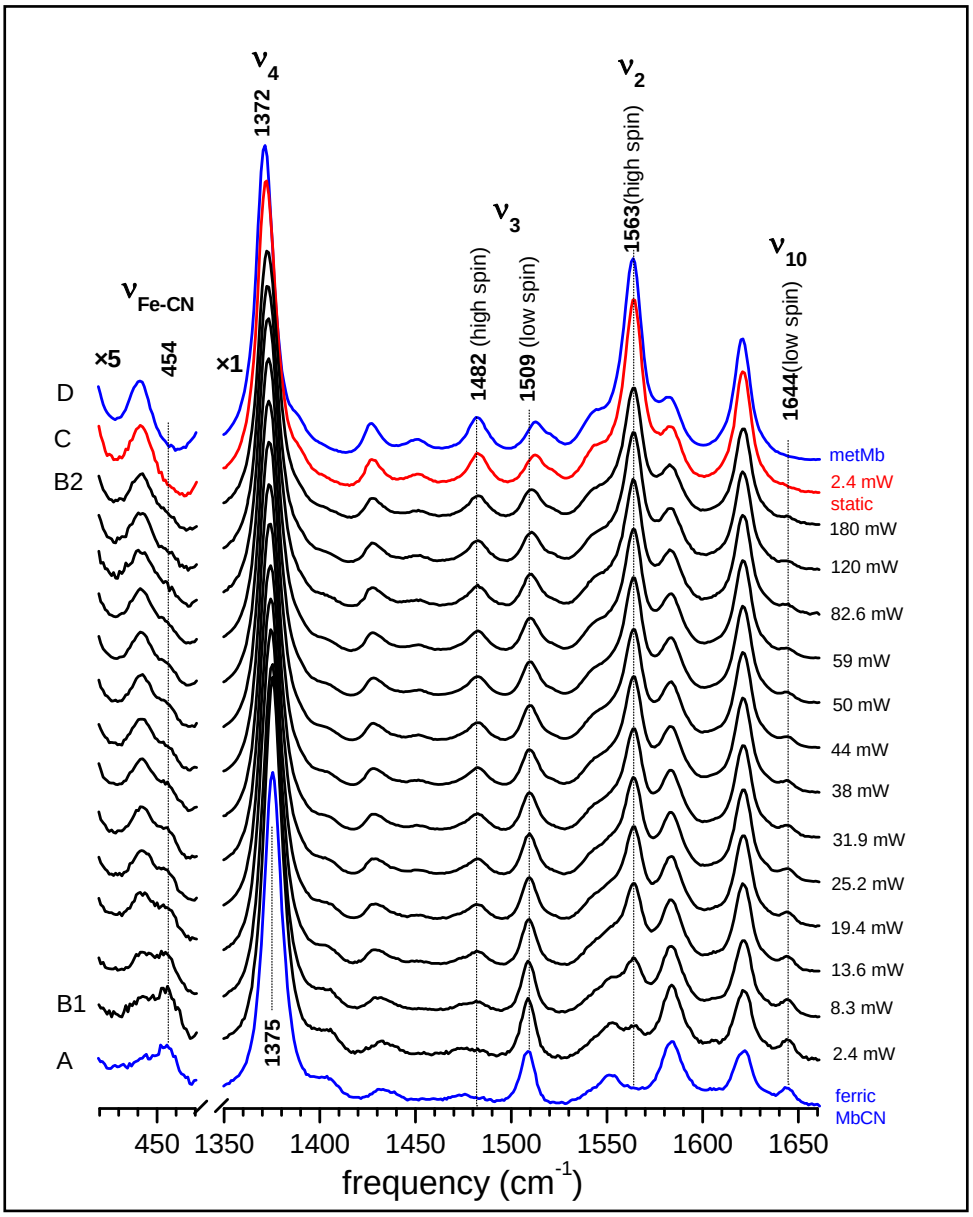

Figure S1: Resonance Raman spectra of ferric MbCN in 0.1M, pH=7.4 potassium phosphate buffer. The concentrations of horse myoglobin and potassium cyanide are 0.05 mM and 0.5 mM, respectively. UV-Vis absorption indicated complete formation of ferric MbCN. To obtain the Raman spectra, the protein solution was spun at 1500 rpm in a quartz cell (10 mm inner diameter). The spectrum for static sample (2.4 mW) is shown in red. Two clean spectra of ferric MbCN (0.07 mM with 50 fold KCN added, 3.4 mW, spin) and metMb (0.07 mM, 24 mW, spin) are also shown (in blue) as references. The excitation wavelength was 413.1 nm and the power was varied as indicated to the right of each spectrum. All spectra are normalized by dividing the spectral intensity by the product of excitation power and accumulation time.

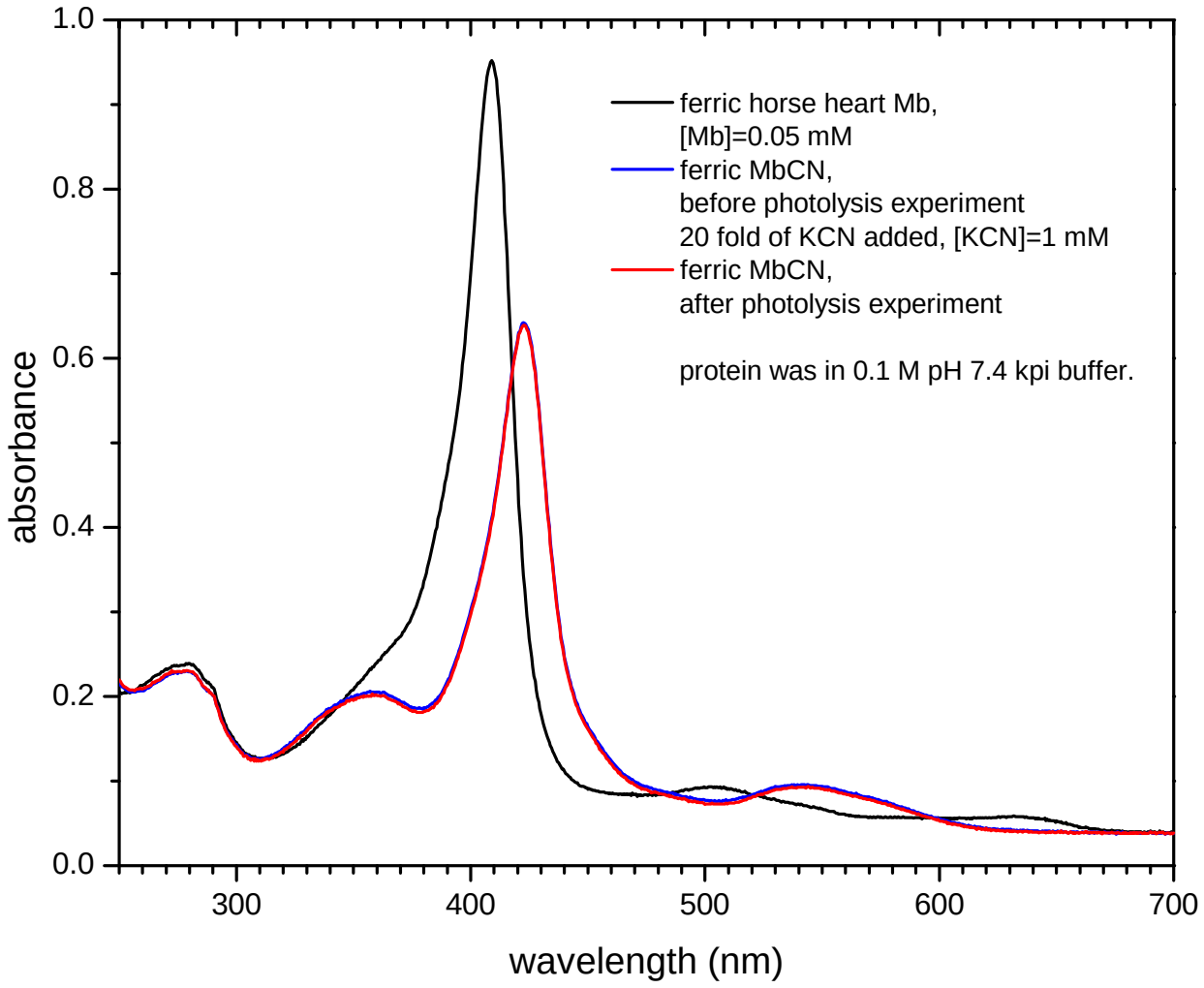

Figure S2: UV-Vis absorption spectra for metMb and ferric MbCN. The black curve was the 0.05 mM metMb in 0.1 M pH 7.4 potassium phosphate buffer. Adding 20 fold of KCN to the metMb solution resulted in the ferric MbCN (blue curve). The red curve was the ferric MbCN after Raman experiments. The consistency between the blue and red spectra indicates that there was no observable photoreduction or other changes to the sample during the Raman measurements.

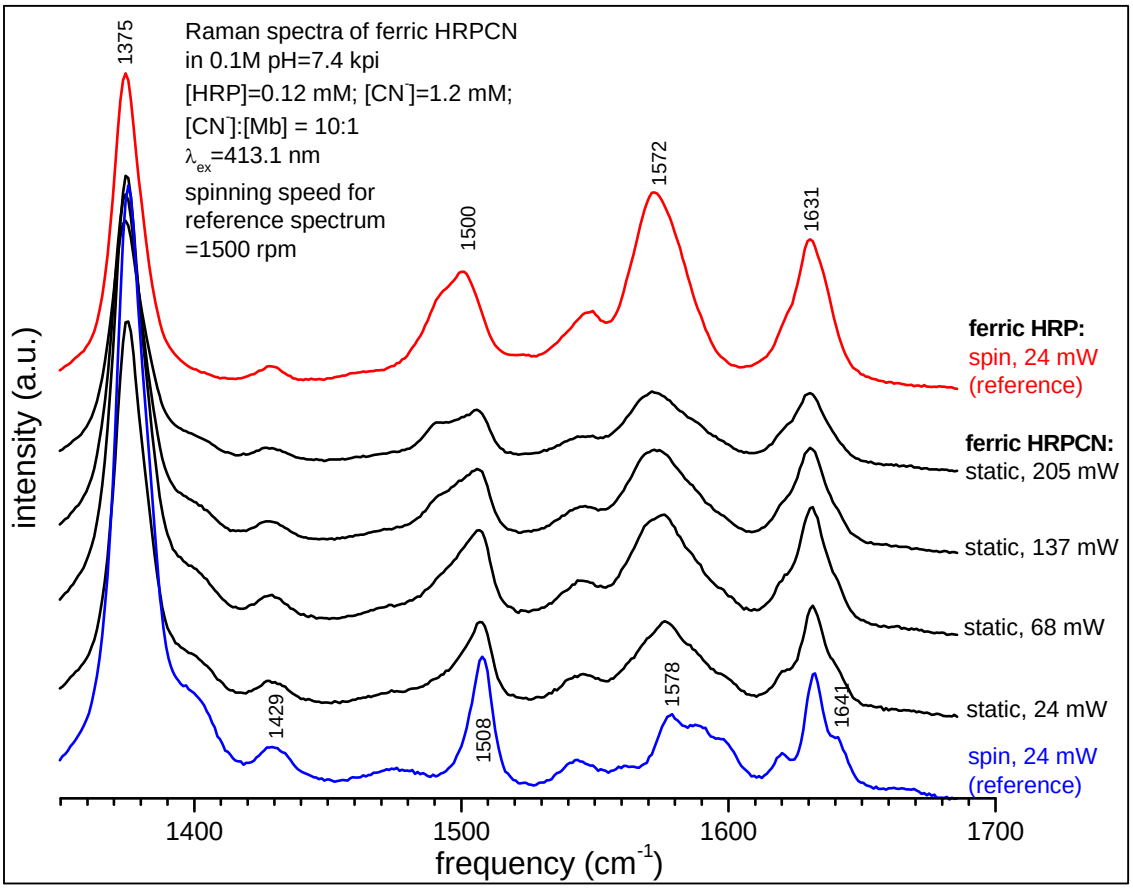

Figure S3: Resonance Raman spectra of ferric horseradish peroxidase (HRP) CN in 0.1M, pH = 7.4 potassium phosphate buffer. The concentrations of HRP and potassium cyanide are 0.12 mM and 1.2 mM, respectively. UV-Vis absorption indicated complete formation of ferric HRPCN. Measurements under spinning conditions (blue spectrum at bottom of figure) show no photolysis because the CN bimolecular binding rate [1] is 9×10^4 $M^{-1}s^{-1}$, roughly 1000 times faster than for CN to metMb. To obtain Raman spectra showing photolysis, the protein solution was measured when the quartz cell (10 mm inner diameter) was static. The spectrum for a pure sample of ferric HRP (24 mW) is shown in red (top spectrum). Spectra of ferric HRPCN under varying power conditions show the evolution of the spectrum from the fully bound to the dissociated state. The ratios of HRP/HRPCN are found to be 0.65, 0.91 and 1.25 for the 24, 68, and 137 mW conditions, respectively. These ratios are smaller than would be expected using the values of k_{BA}, k_{out}, and Y = 0.75 found for MbCN and the drop-off with increasing power suggests that convection processes in the stationary cell may be responsible for increased HRPCN not accounted for in the simple kinetic model. The excitation wavelength was 413.1 nm and the power was varied as indicated to the right of each spectrum. All spectra are normalized by dividing the spectral intensity by the product of excitation power and accumulation time.

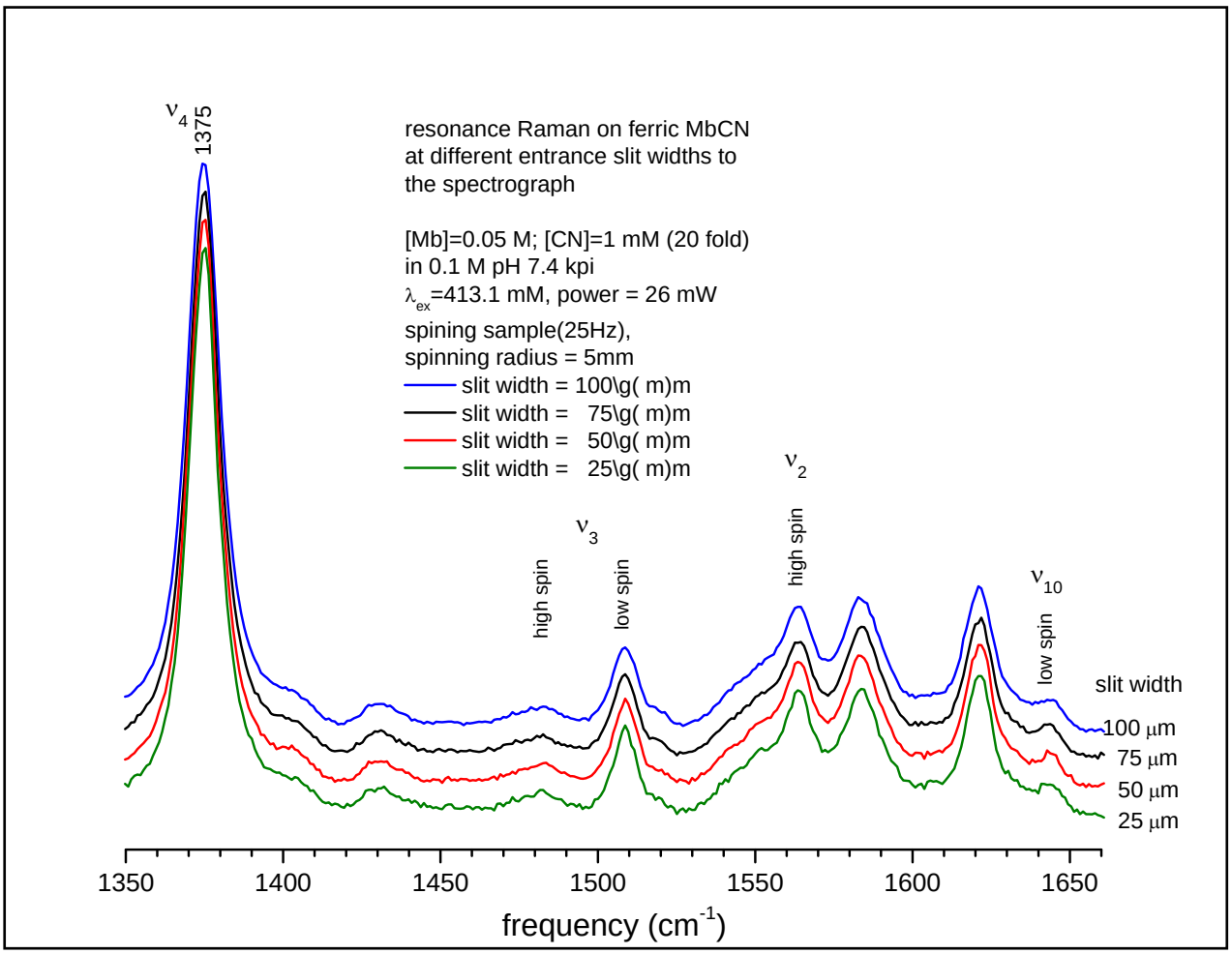

Figure S4: No apparent change in the ratio of MbCN to metMb was observed as the monochromator slit-width was varied. This indicates that no significant spatial variation of the population ratio due to diffusion in the angular direction is taking place.

II. Diffusion Estimates

We estimate the diffusion of the MbCN photolysis product (met Mb) out of, and the diffusion of unphotolyzed MbCN into, the laser focal region that is imaged into the monochromator entrance slit and detected. To do this, we have to solve the reaction-diffusion equation:

$$du/dt = D\nabla^2 u - k_{CA}u \qquad \text{(S1)}$$

The detectable region is defined by a height, h (on the order of 1-2 mm), over which secondary radiation emits from the sample and passes through the monochromator entrance slit. There is also a width $\pm w_1$, within which Raman signal can pass through the monochromator's entrance slit. The quantity $2w_1$ is found by projecting the monochromator slit width back through the magnification of the collection and focusing lenses, which in this case is simply the ratio of their focal lengths $M=f_1/f_2=6/1$. The attenuation of the laser beam as it passes upward through the sample in the z direction can be handled by treating each slice in the vertical direction, Δh, independently.

Here our discussion is limited to the situation where the sample solution reaches a photostationary state equilibrium, i.e. the observed metMb population in the resonance Raman experiment is fixed for a given laser power and sample spinning rate. In order to solve the problem, let us consider a slice of the MbCN solution centered in the laser beam at the bottom of the quartz cylinder with height Δh, and small width given by an angle $\Delta\theta$ and the cell radius R=5mm ($R\Delta\theta$), which rotates at an angular speed ω around the center line of the quartz cylinder. Prior to radial diffusion taking place as the sample rotates through the dark part of its cycle in the spinning cell, the initial met Mb radial distribution can be written as:

$$u_{di} = \frac{N_{met}}{\sqrt{2\pi}\sigma_{met}\Delta h R\Delta\theta}\exp\left(-\frac{(r-r_0)^2}{2\sigma_{met}^2}\right) \qquad \text{(S2)}$$

where σ_{met} is the width of the assumed Gaussian distributed metMb population at the end of light phase and the beginning of dark phase, N_{met} is total number of molecules of metMb in that slice and r_0 locates the center of the Gaussian distribution, which is also the center of the laser focus spot.

The solution for reaction-diffusion equation is rather complicated, even under simple boundary conditions. However, for the one-dimensional problem with no boundary, and initial condition $u(r,0) = u_{di}(r)$, the solution is rather simple:

$$u(r,t) = \frac{e^{-k_{CA}t}}{2\sqrt{\pi Dt}}\int_{-\infty}^{\infty} u_{di}(r')\exp\left(-\frac{(r-r')^2}{4Dt}\right)dr' \qquad \text{(S3)}$$

Using the Gaussian distributed initial condition, eq. (S3) can be written as:

$$u(r,t) = \frac{e^{-k_{CA}t}N_{met}}{\sqrt{2\pi}\sigma(t)\Delta h\Delta\theta R}\exp\left(-\frac{(r-r_0)^2}{2\sigma(t)^2}\right), \qquad \sigma(t) = \sqrt{\sigma_{met}^2 + 2Dt} \qquad \text{(S4)}$$

When the system reaches equilibrium, the variation of the relative population is very small in the angular direction. We estimate that, at 1 mM CN and 10 mW power, the percentage loss of [metMb] from the detected region (along the angular direction) during the dark phase goes as $-k_{CA}\tau \sim 0.68\%$. Correspondingly, the [metMb] increases by the same amount during the photodriven light phase as must occur under photostationary conditions. Thus, it is reasonable to assume that diffusion plays a minor role along the angular coordinate.

Under photostationary equilibrium conditions along the radial coordinate we assume $du/dt = 0$ in order to estimate σ_{met}. When we do this calculation in the radial direction, the width of the metMb distribution just after the light phase is found to be roughly 3 times that of the laser beam width $\sigma_L = 0.85 r_L = 8.5$ μm that is driving the photophysics of met formation. Here the beam radius, r_L, is defined as one-half the full-width at half maximum of the Gaussian beam profile, while σ_L is the width at which intensity has dropped by $e^{-0.5}$=0.607.

The point source solution is:

$$u(r) = u_{r'}e^{-|r-r'|/\sigma_{met}}, \qquad \text{(S5)}$$

With $\sigma_{met} = \sqrt{D/k_{on}}$. Since $k_{CA} = 0.17s^{-1}$ and $D = 1.0 \times 10^{-6} cm^2 s^{-1}$ [2], we have $\sigma_{met} = 24\ \mu m$. Considering that the incident laser is centered at r_0 and keeps pumping metMb into solution, the complete photostationary state solution should be the convolution of eq. (S5) with the photon flux distribution. Thus we have:

$$\begin{aligned} u(r) &= \frac{u_0}{\sqrt{2\pi}\sigma_L}\int_0^R dr' \exp\left(-\frac{(r'-r_0)^2}{2\sigma_L^2}\right)e^{-\frac{|r-r'|}{\sigma_{met}}} \\ &= \frac{u_0}{2\sqrt{2}}\exp\left(\frac{\sigma_L^2}{2{\sigma_{met}}^2} - \frac{r-r_0}{\sigma_{met}}\right)\left(1-\mathrm{erf}\left(\frac{\sigma_L}{\sqrt{2}\sigma_{met}} - \frac{r-r_0}{\sqrt{2}\sigma_L}\right)\right) \\ &\quad + \frac{u_0}{2\sqrt{2}}\exp\left(\frac{\sigma_L^2}{2{\sigma_{met}}^2} + \frac{r-r_0}{\sigma_{met}}\right)\left(1-\mathrm{erf}\left(\frac{\sigma_L}{\sqrt{2}\sigma_{met}} + \frac{r-r_0}{\sqrt{2}\sigma_L}\right)\right) \end{aligned} \qquad \text{(S6)}$$

Where we have closed the integral by assuming the integrand decays prior to encountering a boundary. The final value of $u(r)$ has a bell-like shape and is symmetric about r_0, so we can use a Gaussian shape function to mimic $u(r)$, and we find the overall width remains near $\sigma_{met} = 24\ \mu m$. This is roughly 3 times the width of the laser beam $\sigma_L = 8.5\ \mu m$.

Since the concentration gradient is very steep along r and varies on a scale of $24\ \mu m$, this dimension presents the major avenue for diffusional effects that might alter the simple photolysis and rebinding population dynamics outlined in the main text. The z-direction concentration

gradient is governed by the length scale of the laser flux attenuation. This is roughly 1 OD in a 1 mm path length, yielding a length scale of ~ $e^{-z/500\mu m}$, which is much larger than the $24\ \mu m$ radial concentration gradient given by Eqs.(S5-S6). Angular diffusion effects are negligible in the photostationary state because the system has less than a ~1% concentration gradient variation around the outer perimeter.

The actual diffusion process within the cylindrical cell involves certain boundary conditions. For this simple treatment, we have assumed the whole laser illuminated area near the focal point lies within the cylindrical cell. For example, we assume $R - r_0 \sim 3\sigma_{met} = 72\ \mu m$, and take the O.D.=1 for 1 mm pathlength and ignore the reabsorption of the Raman signal. Under these reasonable conditions, we find that the above solution remains an acceptable approximation. It is worth mentioning that, because the solution is symmetric about r_0 , eqs. (S4) and (S6) are the exact solutions for the problem with a boundary at $r = r_0$ and r in the range $(0, r_0)$.

The resonance Raman signal contributed by the metMb population in the solution is the integration of the metMb concentration over the volume of the incident light that is imaged into the monochromator. We take a Gaussian volume that mimics the laser beam profile and let r_L = $1.18\sigma_L$=10μm be the radius of the laser focal spot. Using Eq. (S4), the time dependent population of metMb contributing to the intensity of the Raman signal for the slice of solution we selected is proportional to the following quantity:

$$P(t) = \frac{e^{-k_{CA}t}}{\sqrt{2\pi}\Delta h \Delta\theta R\sigma(t)} \int_{slice} dhRd\theta dr \exp\left(-\left(\frac{1}{2\sigma(t)^2} + \frac{1}{2\sigma_L^2}\right)(r - r_0)^2\right)$$
$$= \frac{e^{-k_{CA}t}}{\sqrt{1 + \sigma(t)^2/\sigma_L^2}} \qquad \text{(S7)}$$

So the measured rate of diffusion can be written as:

$$\frac{dP}{dt} = -k_{CA}P - \frac{D}{\sigma_L^2 + \sigma(t)^2}P = -k_{CA}P - k_{diff}P, \qquad \text{(S8)}$$

In which, $k_{diff} = D/(\sigma_L^2 + \sigma(t)^2)$. Since $2DT \sim 0.05(\mu m)^2 \ll \sigma_L^2, \sigma_{met}^2$, we estimated $k_{diff} \sim 0.14 s^{-1}$. Thus the total effective rate for loss of the metMb population being probed can be crudely defined as $k_{eff} \equiv k_{CA} + k_{diff} \sim 2k_{CA} \sim 0.3 s^{-1}$ when [CN]=1 mM.

On the other hand, the experiments performed with two different cyanide concentrations yield results that suggest k_{diff} is negligible comparable to k_{CA}. The discrepancy between the above theoretical estimates and the experimental evidence that diffusion is negligible can be attributed to the approximation where we used a steeper Gaussian-shaped metMb concentration profile than the actual distribution given by eq.(S6) to estimate σ_{met}. If the true value of σ_{met} is increased by just a factor of 2, the effective contribution due to diffusion drops by a factor of ~4. Thus, we rely on the experimental test using different concentrations of CN to deduce that radial diffusion of MbCN into the laser focal region is playing a very minimal role in the population

recovery, even though the rates are slow enough that we need to be cautious about this possibility.

III. Entrance slit width effect

In the previous section, we discussed the diffusion during the dark phase. During the light phase, the concentration of metMb can be described as

$$u(r,t) = u(r,0) + \Delta u(r,t),$$

$$\Delta u = \sqrt{2}\, k_{off} t_\sigma \big(u_a - u(r,0)\big) \exp\left(-\frac{(r-r_0)^2}{2\sigma_L^2}\right)\left(1 + \frac{2}{\sqrt{\pi}}\mathrm{erf}\left(\frac{t-t_0}{\sqrt{2}t_\sigma}\right)\right) \qquad \text{(S9)}$$

where $t_\sigma = \sigma_L/\omega R \sim 10.6\ \mu s$, u_a is the sum of [metMb] and [MbCN], which is a constant, and t_0 is the time when the selected slice passes the center of the laser focal spot.

The Raman signal coming from the sample solution which passes through the entrance slit ($\pm w$) of the monochromator is the sum of the signals from all slices within $\pm w$. Thus the signal is proportion to:

$$S \propto \int_{-w/R}^{+w/R} d\theta \int_0^R dr\ (u(r,0)I(r,\theta) + \Delta u(r,\theta/\omega + t_0)I(r,\theta)) \qquad \text{(S10)}$$

Where photon flux profile: $I(r,\theta) \propto \exp(-((r-r_0)^2 + \theta^2 R^2)/(2\sigma_L^2))$, and ω is the angular speed of quartz cylinder. Here we assume center of laser focus spot is at angle 0°, and ignore the reabsorption of the Raman signal.

As previously estimated, the concentration gradients along θ are much smaller than the gradients along the radial direction. Since Δu is only ~0.68% of u along the angular direction at 10 mw incident laser power, we don't expect any observable change from eq.(S10), when we vary the monochromator slit width, $2w$. Thus, the diffusion along the θ direction is not observable by varying the slit width (Fig. S4).

References

(1) Ellis, W. D.; Dunford, H. B. The Kinetics of Cyanide and Fluoride Binding by Ferric Horseradish Peroxidase. *Biochemistry* **1968,** *7*, 2054-2062.
(2) Riveros-Moreno, V.; Wittenberg, J. B. The Self-Diffusion Coefficients of Myoglobin and Hemoglobin in Concentrated Solutions. *J. Biol. Chem.* **1972,** *247*, 895-901.